Continuum Mech. Thermodyn. (2020) 32:421–432
https://doi.org/10.1007/s00161-019-00788-w

ORIGINAL ARTICLE

Rebecca Jennrich · Alexander Lion · Michael Johlitz · Sarah Ernst · Klaus Dilger · Elisabeth Stammen

Thermomechanical characterization and modeling of fast-curing polyurethane adhesives

Received: 14 November 2018 / Accepted: 12 May 2019 / Published online: 17 May 2019

Abstract In the context of lightweight design and modern hybrid technologies, the importance of structural and soft adhesives in industrial applications is increasing. Therefore, this paper examines a relatively soft polyurethane adhesive characterized by showing nonlinear viscoelastic behavior at room temperature and enduring large deformations. It is well suited for applications under dynamic loadings and can compensate gap changes generated by materials with different thermal expansion coefficients. Theoretically, the examined one-component polyurethane adhesive can be cured either thermally or through humidity, resulting in the same mechanical characteristics. Comparing both curing reactions, humidity curing is much slower than thermal curing. The latter can be controlled through the temperature, which may be applied through heating rates of up to 150 K min^{-1}. However, in comparison with metals polyurethane conducts the heat with a much smaller rate which results in high temperature gradients within the adhesive layer. This paper focuses on the modeling of a fast-curing polyurethane adhesive under consideration of the changes in density and thermomechanical material properties induced by thermal curing. Therefore, the material properties need to be observed throughout the thermal curing process, from the uncured fluid to the cured rubber material. In the long term, the accurate prediction of the materials behavior will ultimately facilitate the optimization of the curing process.

Keywords Curing · Caloric experiments · Viscoelasticity · Thermomechanics · Material modeling · Polyurethane

1 Introduction and state of the art

Polyurethane adhesives cure through a polyaddition reaction. Typically, the reaction of one-component polyurethane adhesives is triggered by humidity diffusing into the adhesive and reacting with the isocyanate-terminated polyurethane pre-polymer. A polyurethane urea is formed. Two-component polyurethane adhesives cure in different ways. Depending on the type of hardener urethanes, urea or—at higher temperature—allophanate can be formed. One-component polyurethanes with a so-called latent hardener cure under temperature influence, releasing the embedded hardener to react with the pre-polymer. The examined one-component adhesive combines thermal curing with moisture-curing mechanisms. Depending on the heating rate and the thickness of the material, thermal curing forms within several minutes to an hour. With no heat activation, the humidity curing forms from the surface into the material at rates of approximately 1 mm within 24 h.

Communicated by Michael Johlitz, Lucien Laiarinandrasana, Yann Marco.

R. Jennrich (✉) · A. Lion · M. Johlitz
Institute of Mechanics, Bundeswehr University Munich, Werner-Heisenberg-Weg 39, 85579 Neubiberg, Germany
E-mail: rebecca.jennrich@unibw.de

S. Ernst · K. Dilger · E. Stammen
Institute of Joining and Welding, Technische Universität Braunschweig, Langer Kamp 8, 38106 Brunswick, Germany

In the works of Yagimli [19] and Liebl [10], the material model is based on an epoxy adhesive. Epoxies cure through a polyaddition reaction similar to polyurethanes. The reaction can be accelerated through heat as well. However, humidity does not affect the reaction itself. Since the humidity reaction of the examined polyurethane adhesive is very slow compared to the thermal reaction, it is neglected when modeling the thermal reaction. Hence, the approach of Yagimli and Liebl is applicable to the polyurethane adhesive. Both works use differential scanning calorimetry (DSC) to study the exothermal curing process as was already described in a paper of Kamal and Sourour [17]. They introduce a phenomenological variable to describe the progress of the reaction and density measurements based on Archimedes' principle to describe the changes in density resulting from the curing reaction as well as temperature changes. The time–temperature-transformation diagram which was proposed by Enns and Gillham [3] is a means to visualize the phase changes during isothermal polymerization. The transition from fluid to solid is incorporated into Liebl's rheological material model for small deformations by formulating the equilibrium spring stiffness of the generalized Maxwell partial model dependent on the degree of curing. That way, the material behavior is viscous below the gel point and viscoelastic with the stiffness increasing with the degree of curing above it. Yagimli considers the impact of the curing reaction on the material behavior for large deformations by formulating the Helmholtz free energy split into a mechanical and a thermal part, both dependent on the degree of curing. In the course of this project, similar approaches will be applied to the characterization of the polyurethane adhesive. In an earlier work of Lion and Höfer [12], the authors propose an approach for the representation of curing in continuum mechanics. The modeling equations are derived from the Helmholtz free energy using a multiplicative split of the deformation gradient and an additive split of the stress power, thus securing thermodynamic consistency. The representation of the progression of curing through an internal state variable is applied as well. The framework of their material model would still be valid, even if different equations for the curing variable are used, so a similar approach may be applied to the material at hand. Adolf and Chambers [1] propose a thermodynamically consistent modeling approach for nonlinear viscoelastic behavior of curing thermosets using the Helmholtz free energy formulation as well. Over the course of several papers, Hossain, Possart and Steinmann describe the modeling of thermosets, first for small strains [6] and then for finite deformations [7]. The small-strain model includes the representation of elasticity and viscoelasticity one- and three-dimensional, a cure-dependent variable and shrinkage following the curing reaction. In [7], the authors formulate a simulation framework for a purely elastic material model using the Neo-Hooke model and the 21-chain model as examples. The material model developed by Rabearison, Jochum and Grandidier [15] describes the curing of an epoxy using a cure kinetics model of the Kamal–Sourour type extended by an additional term for diffusion effects. The experimental investigations include mainly DSC experiments under constant temperature or constant heating. An approach similar to the diffusion-controlled part of an epoxy's curing reaction may be used to describe the polyurethane's curing through humidity. In [13], Mahnken developes a material model for viscoelasticity at large deformations considering curing, for which the author then demonstrates thermodynamic consistency for typical load cases. The volumetric changes are split into an effective part stemming from mechanical loading, a thermal part from changes in temperature and a chemical part from the curing reaction. This distinction, except the mechanical part, will be implemented into the polyurethane material model as well. The application of density measurements using Archimedes' principle and the subsequent identification of a cure kinetics model of the Kamal–Sourour type for epoxy resin using only density measurement data is described by Leistner et al. [8]. In another publication, Leistner et al. [9] examined the Kamal–Sourour model and an extension for diffusion-controlled curing proposed by Fournier et al. [4] concerning the correlation between different parameters and the over-parametrization of material models. The models are subsequently modified and used in studies regarding the stability of the ODE and convergence using first-, second- and third-order integration schemes and a wide range of constant timesteps. These studies are of particular interest to us and may be applied to the cure kinetics model proposed in Sect. 3 in the future.

2 Experimental observations

To be able to predict the material behavior under various conditions like thermal or mechanical loadings, it is not necessary to observe the behavior under exactly the same circumstances, but rather choose significant experiments as cornerstones for the material model. For the material at hand, the behavior can be split into a predominantly mechanical and a predominantly thermochemical part, each of which may be investigated individually. The relevant material parameters for the mechanical part of the model have been identified as the elastic Yeoh parameters c_{10}, c_{20} and c_{30} [21] and the viscoelastic parameters τ and μ, which constitute the

dashpot's viscosity and the spring's stiffness in a rheological Maxwell element [11]. For the thermochemical part, there are the curing reaction enthalpy and the thermal expansion coefficients, the specific heat capacity and the thermal diffusivity and conductivity, respectively. Through cleverly chosen test conditions, the experimental costs can be kept to a minimum. The resulting parameters are collected in Tables 1 and 2. The first step is the examination of the curing reaction itself, which may depend on temperature and humidity. Most material parameters need to be identified for the uncured and the fully cured material separately. Furthermore, the correlation between these parameters and the degree of curing has to be identified also. In the following section, the different experiments will be described in detail.

2.1 Curing

To define the state of the material related to the curing reaction, the degree of curing is introduced as an internal state variable. It is symbolized by the letter q and ranges from zero for the uncured material to one for the fully cured material. Since the degree of curing significantly affects not only the thermal, but also the mechanical material behavior, it will be identified first. The chemical reaction that describes the transition from fluid to solid is the forming of a urea network through the reaction of amine groups with isocyanate under the release of carbon dioxide. Elevated temperatures accelerate this process. The curing reaction is investigated using differential scanning calorimetry, which allows us to quantify the difference in enthalpy between a specimen and a reference that are exposed to the same temperature program. Phase transitions like crystallization and melting as well as the glass transition can be observed as exothermal or endothermal processes in the specific enthalpy rate signal. For the purpose of examining the reaction enthalpy of curing, the specimen is exposed

Table 1 Material parameters gained from the caloric experiments

Parameter	Symbol	Experiment	Value
Glass transition temperature ($q = 0$, previous cooling rate $-10\,\mathrm{K\,min^{-1}}$)	T_{g0}	DSC	$-72\,^{\circ}\mathrm{C}$
Glass transition temperature ($q = 1$, previous cooling rate $-10\,\mathrm{K\,min^{-1}}$)	T_{g1}	DSC, TMA	$-66\,^{\circ}\mathrm{C}$
Linear thermal expansion coefficient ($T > T_g$, $q = 0$)	α_0	Archimedes	$19.8 \times 10^{-5}\,\mathrm{K^{-1}}$
Linear thermal expansion coefficient ($T < T_g$, $q = 0 \ldots 1$)	α_1	TMA	$6.55 \times 10^{-5}\,\mathrm{K^{-1}}$
Linear thermal expansion coefficient ($T > T_g$, $q = 1$)	α_2	TMA	$12.8 \times 10^{-5}\,\mathrm{K^{-1}}$
Thermal conductivity ($q = 1$)	κ	HotDisk	$0.24\,\mathrm{W\,m^{-1}\,K^{-1}}$
Specific heat capacity at constant pressure ($q = 0$)	c_{p0}	DSC	$1.55\,\mathrm{J\,g^{-1}\,K^{-1}}$
Specific heat capacity at constant pressure ($q = 1$)	c_{p1}	DSC	$0.42\,\mathrm{J\,g^{-1}\,K^{-1}}$

Table 2 Material parameters gained from the mechanical experiments

Parameter	Symbol	Value
Equilibrium spring stiffness parameters identified at 20 °C	c_{10}	$169.1 \times 10^{-3}\,\mathrm{MPa}$
	c_{20}	$16.5 \times 10^{-3}\,\mathrm{MPa}$
	c_{30}	$17.7 \times 10^{-6}\,\mathrm{MPa}$
Maxwell spring stiffness parameters identified at 20 °C	μ_1	0.10 MPa
	μ_2	0.70 MPa
	μ_3	0.17 MPa
	μ_4	0.12 MPa
	μ_5	0.15 MPa
	μ_6	1.20 MPa
	μ_7	0.18 MPa
Maxwell dashpot relaxation time parameters identified at 20 °C	τ_1	3.88 s
	τ_2	30.00 s
	τ_3	1.13×10^{3} s
	τ_4	1.16×10^{4} s
	τ_5	1.00×10^{8} s
	τ_6	1.00×10^{10} s
	τ_7	1.01×10^{12} s
WLF parameters	W_1	6.2216
	W_2	221.9566 K

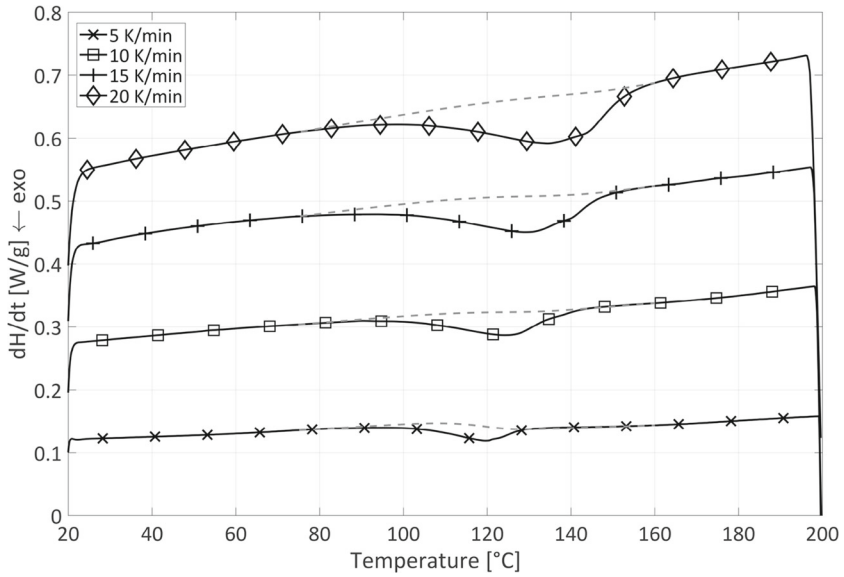

Fig. 1 DSC measurement curves from the curing cycle with different heating rates

to a three-part temperature program under a protective gas atmosphere. In the first cycle, the curing cycle, the temperature is increased linearly from room temperature up to the maximum temperature of 200 °C. To ensure that the curing finished completely within the first cycle and that no degradation of the material happens, the second and third cycles are validation cycles, where the specimen is first cooled down to −110 °C with a constant cooling rate and subsequently heated up to 200 °C again. If the signals of the two validation cycles show no exothermal curing peak and are otherwise identical as well, it is proven that the curing cycle contains the complete curing reaction and can be used to determine the reaction enthalpy. The experiment is repeated with different constant heating rates in the curing cycle, see Fig. 1. The exothermal reaction peak is separated from the specific enthalpy rate signal of the curing cycle conforming to standards [2] (Fig. 2) and used to compute the degree of curing q following Eq. 1, where H is the specific enthalpy and H_{total} is the specific enthalpy of the whole curing reaction. The simulation model and parameter fitting for the curing reaction are described in Sect. 3.

$$\dot{q} = \frac{1}{H_{\text{total}}} \frac{\mathrm{d}H}{\mathrm{d}t} \tag{1}$$

For the experiments on fully cured material, the adhesive is cured under defined temperature and humidity conditions in the form of plates or tensile specimens. To examine the effect of the curing temperature on the mechanical properties, 23 °C, 90 °C and 130 °C are chosen as curing temperatures. Furthermore, for the investigation of the diffusion-driven humidity curing, material is cured at 23 °C under 30, 50 and 70% relative humidity. These investigations will be examined in the next publication.

2.2 Caloric behavior

The thermal deformation behavior can be divided into three parts: The first is the thermal deformation of the completely uncured material, the second of the fully cured material and the third concerns the whole spectrum in between. Furthermore, the different states of the material above and below the glass transition temperature (T_{g}) must be taken into consideration. Therefore, the thermal expansion coefficient needs to be identified for fully cured material below T_{g} as α_1, which will be valid for the uncured material as well since the thermal expansion coefficient is said to be independent of the degree of curing in the glassy state, and above the T_{g} for the uncured as α_0 and the fully cured material as α_2, respectively. Identifying the thermal expansion coefficient for the fully cured material, which is basically an elastomer, can be carried out via thermomechanical analysis (TMA). A small specimen is subjected to a temperature program while its length is measured and used to compute the linear thermal expansion coefficients. The temperature program spans a range from −100 to 100 °C, so the coefficients both above and below the glass transition can be identified with just one experiment, see Fig. 3.

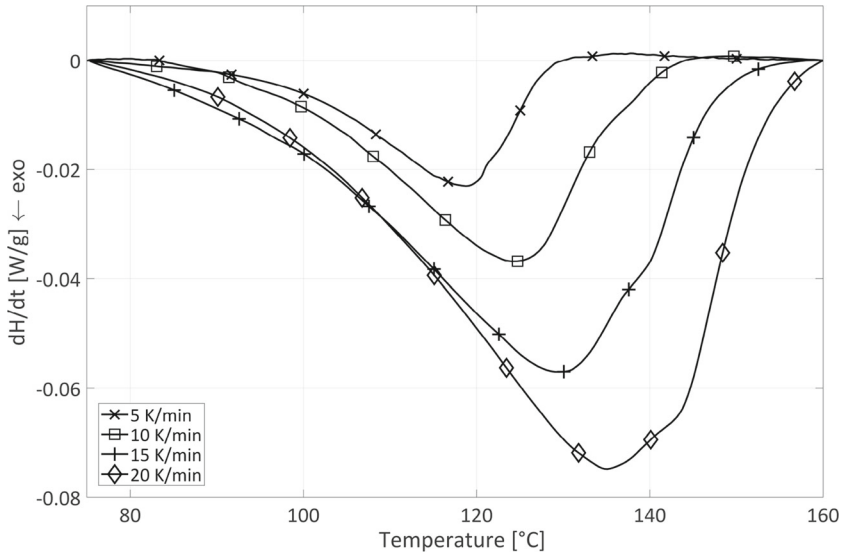

Fig. 2 Exothermal reaction peaks separated from the DSC measuring curves

TMA may not be used with the uncured material since its soft, paste-like texture would not withstand even the probe's small contact force, and hence, a different experimental setup is needed to measure the thermal deformation. Using a fluid with a well-known density over a wide temperature range and assuming constant mass, it is possible to measure the density and volume changes as shown in Fig. 4. Archimedes' principle is based on the changing buoyancy of the sample brought on by volumetric expansion, as can be seen in Eq. 2, where θ is the temperature, ρ_s and ρ_f are the specimen and fluid densities, and m_sa and m_sf are the specimen masses in air and submerged in the fluid. The manufacturer specifies the curing shrinkage as 5%.

$$\rho_\mathrm{s}(\theta) = \frac{m_\mathrm{sa}}{m_\mathrm{sa} - m_\mathrm{sf}(\theta)} \cdot \rho_\mathrm{f}(\theta) \tag{2}$$

The volumetric thermal expansion coefficient can be computed from the density, which may be converted into the linear coefficient, provided that the material is isotropic, following Eq. 3.

$$\alpha_\mathrm{vol} = 3 \cdot \alpha_\mathrm{lin} = \frac{\rho_\mathrm{s0} - \rho_\mathrm{s1}}{\rho_\mathrm{s1} \cdot (\theta_1 - \theta_0)} \tag{3}$$

Following the DSC experiments conducted to quantify the curing reaction enthalpy, the specific heat capacity for the cured and the uncured material can be gained from similar measurements. Using the HotDisk method, where the cured material is locally exposed to a defined calorific output while the temperature on the specimen surface is measured by a resistance thermometer, we get the thermal conductivity κ.

2.3 Mechanical behavior

When characterizing the mechanical behavior of a viscoelastic material, the hyperelastic parameters and the viscoelastic parameters can be investigated separately. To see purely hyperelastic behavior under static loading, we would have to conduct a relaxation test with an infinite relaxation period. The multi-step relaxation test consists of several loading steps with finite relaxation periods in between, and the same number of unloading steps, also with relaxation periods in between. There is a corresponding relaxation point on loading and unloading at the same engineering strain each step. In theory, given enough relaxation time on each step these corresponding points would meet on the so-called equilibrium stress–strain curve, so we gain the equilibrium curve by interpolation. Figure 5 shows the experimental curve as well as the interpolated equilibrium curve with the stress given as the first Piola–Kirchhoff or engineering stress (1. PK). For the viscoelastic parameters, a second relaxation experiment is conducted with impulse-like loading. That way, the full relaxation spectrum may be observed (Fig. 6). The mechanical parameters are fit to a simple generalized Maxwell model. For information on the whole material model, refer to Sect. 3.

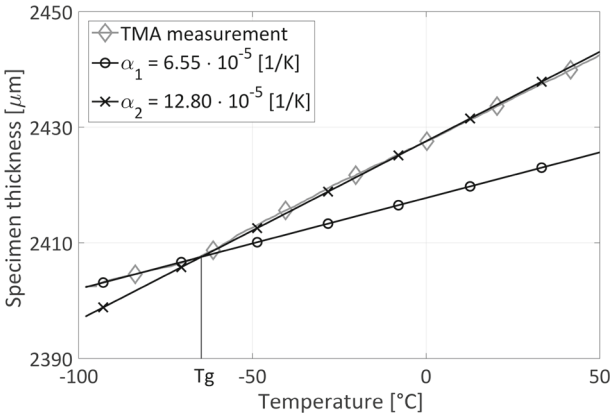

Fig. 3 TMA measuring curves with the thermal expansion coefficient above and below T_g. The material was cured at 130 °C for 10 min

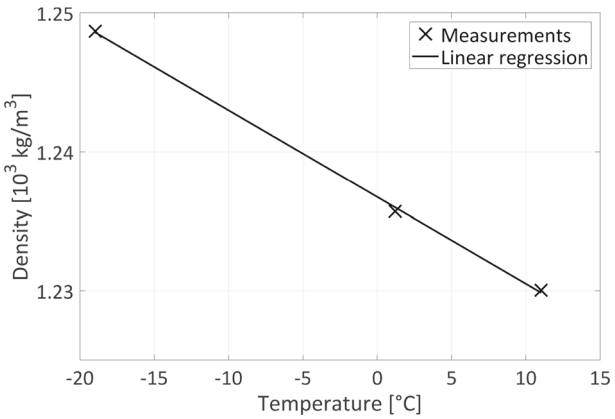

Fig. 4 Change in density over different temperatures in the uncured material

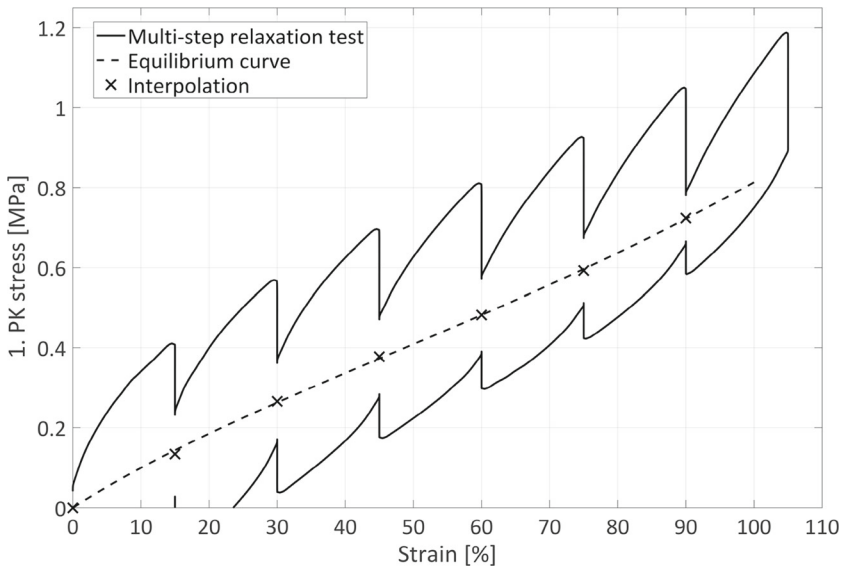

Fig. 5 Multi-step tensile relaxation test with interpolated equilibrium curve. The material was fully cured at 130 °C for 10 min

The viscoelastic material behavior also depends on temperature and frequency, which may be investigated using a dynamic mechanical analysis (DMA). A specimen that was fully cured at 90 °C for 40 min is exposed

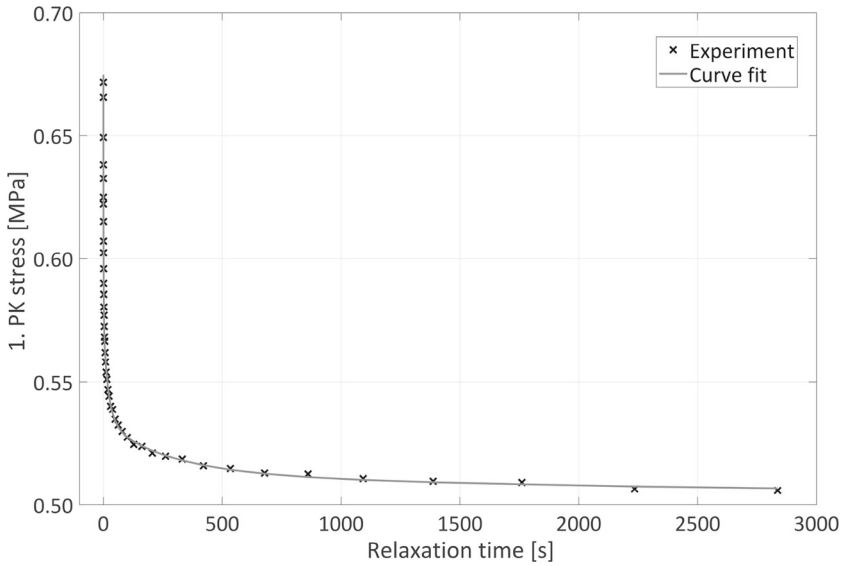

Fig. 6 Relaxation with impulse-like loading. The material was fully cured at 130 °C for 10 min

to cyclic tensile loading at different temperatures from −70 to 130 °C and loading frequencies from 1 to 100 Hz. The small dynamic amplitude guarantees a linear material response. To describe the material behavior over a larger frequency range, we make use of the so-called time–temperature superposition principle. For thermorheologically simple material under small deformations, an experiment at a lower temperature is equivalent to one at a higher frequency. Thus, the results at frequencies too high or too low to be valid for an experiment may be generated by using the time–temperature shift [5]. By shifting the curve fragments gained from DMA experiments at different temperatures along the logarithmic time or frequency axis, the so-called master curve is generated. An equation to use in material modeling may be fit to this master curve, for example one of the two main superposition principles: The Williams–Landel–Ferry (WLF) equation (Eq. 4a) and the Arrhenius equation. The WLF parameters W_1 and W_2 define the way the curve fragments are shifted in relation to the reference temperature with a_T as the so-called shift factor. Though the WLF parameters are said to be constant parameters independent of the chosen material, this is true only for a small time or frequency range of 1.5–2 decades, otherwise the parameters may differ considerably [5]. The time–temperature shift using the WLF equation is intended for a temperature range from T_g to $T_g + 100\,\mathrm{K}$ [18]. The Arrhenius equation contains the activation energy E_0 which a macromolecule has to overcome to change its place inside the material, and the universal gas constant R as well as the shift factor. It is usually used for processes far above the glass transition temperature [14]. When the frequency range exceeds the equations' range of use, a combination of both may improve the result [5]. Figure 7 shows that even though the chosen frequency range far exceeds the WLF equation's range of use (approximately − 65 to 35 °C), it still produces satisfactory results.

$$\log a_\mathrm{T} = -\frac{W_1 \cdot (\theta - \theta_\mathrm{ref})}{W_2 + (\theta - \theta_\mathrm{ref})} \tag{4a}$$

The identified parameters for completely cured material at room temperature are summarized in Table 2.

3 Modeling and identification

For the development of a simplified material model, a common approach is the combination of rheological elements. The linear one-dimensional material model shown in Fig. 8 can be separated into a thermomechanical part (left) and a thermochemical part (right). The thermomechanical part consists of the equilibrium spring connected in parallel with seven Maxwell elements, each of which is made up of one spring and one dashpot connected in series. The thermochemical part consists of two expansion elements to account for the thermal expansion and the chemical shrinkage. The deformation contributions of the thermochemical part are purely volumetric and only consider changes in temperature and degree of curing. They may be neglected

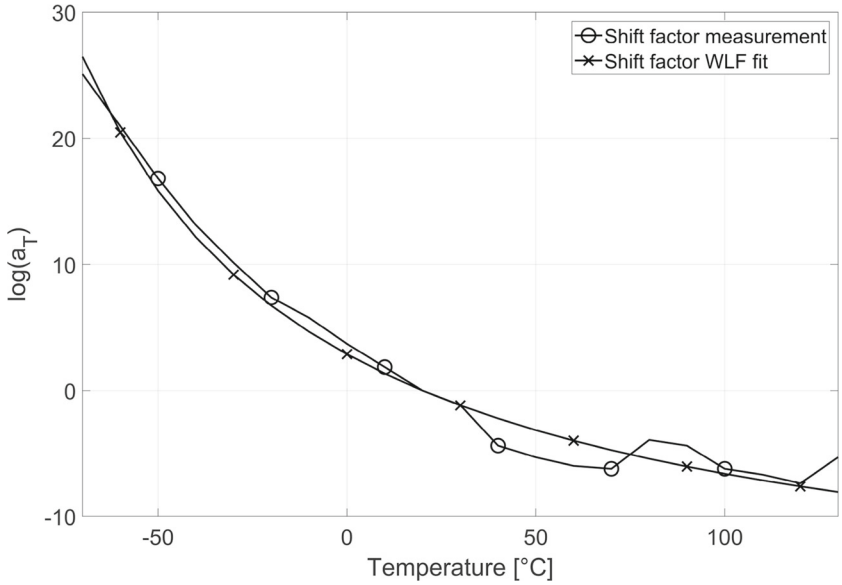

Fig. 7 Shift factor used in the measurement data and shift factor fit with the WLF equation

when identifying the mechanical parameters under isothermal conditions for the completely cured material. Consistent with the hyperelastic deformation behavior observed in the multi-step relaxation test in Fig. 5 at higher strains, the equilibrium spring is modeled using a hypoelastic formulation of the Yeoh model valid for uniaxial stress processes for mechanically incompressible materials (Eq. 5), so that the equilibrium stiffness can evolve stress-free with the degree of curing [6]. The parameters $c_{10}(q)$, $c_{20}(q)$ and $c_{30}(q)$ are the Yeoh model's equivalent of the elastic modulus, λ is the stretch and $\tilde{T}_{\mathrm{eq}}$ the equilibrium stress. The Maxwell elements are each characterized by the elastic spring's stiffness μ and the relaxation time $\tau(q,\theta)$. The inelastic stretch λ_{in} for each Maxwell element is computed according to Eq. 6a, where the exponent n denotes the solution at the time t_n, the exponent $n+1$ at the time t_{n+1}, respectively. That approach has already been proposed by Shutov, Landgraf and Ihlemann [16], who derive the relationship for the inelastic stretch under uniaxial loading shown in equation 6a from the formulation of the right Cauchy–Green strain tensor $\mathbf{C}$, which leads to the implicit solution in one step. Using the inelastic stretch the non-equilibrium stress $\tilde{T}_{\mathrm{neq}}$ is computed for each Maxwell element (Eq. 6b). The total stress $\tilde{T}$ is the sum of the equilibrium stress and the non-equilibrium stress of each Maxwell element, as can be seen in Eq. 6c. The parameters were fit using the MATLAB standard functions lsqnonlin (least squares) and ga (genetic algorithm). The identified parameters for the thermomechanical part of the model (elastic parameters c_{10}, c_{20} and c_{30} and the Maxwell spring stiffnesses μ_i and dashpot relaxation times τ_i) at 20 °C for the fully cured material are available in Table 2.

$$\begin{aligned}\dot{\tilde{T}}_{\mathrm{eq}} = {} & 2\left(2c_{20}(q)\left(2\lambda\dot{\lambda}-\frac{2\dot{\lambda}}{\lambda^2}\right)+3c_{30}(q)\left(2\lambda\dot{\lambda}-\frac{2\dot{\lambda}}{\lambda^2}\right)2\left(\lambda^2+\frac{2}{\lambda}-3\right)\right)\left(\lambda-\frac{1}{\lambda^2}\right)\\ & +2\left(c_{10}(q)+2c_{20}(q)\left(\lambda^2+\frac{2}{\lambda}-3\right)+3c_{30}(q)\left(\lambda^2+\frac{2}{\lambda}-3\right)^2\right)\left(\dot{\lambda}+\frac{2\dot{\lambda}}{\lambda^3}\right)\end{aligned} \tag{5}$$

$$\lambda_{\mathrm{in}}^{n+1} = \sqrt[2]{\left(\left(\left(\lambda_{\mathrm{in}}^{n}\right)^2+\frac{2dt\lambda^2}{\tau(q,\theta)}\right)\left(\frac{1}{\lambda_{\mathrm{in}}^{n}}+\frac{2dt}{\lambda\tau(q,\theta)}\right)^2\right)^{-\frac{1}{3}}\left(\left(\lambda_{\mathrm{in}}^{n}\right)^2+\frac{2dt\lambda^2}{\tau(q,\theta)}\right)} \tag{6a}$$

$$\tilde{T}_{\mathrm{neq}} = \mu\left(\frac{\lambda}{\left(\lambda_{\mathrm{in}}^{n+1}\right)^2}-\frac{\lambda_{\mathrm{in}}^{n+1}}{\lambda^2}\right) \tag{6b}$$

$$\tilde{T} = \tilde{T}_{\mathrm{eq}}+\sum_{m=1}^{7}\tilde{T}_{\mathrm{neq},m} \tag{6c}$$

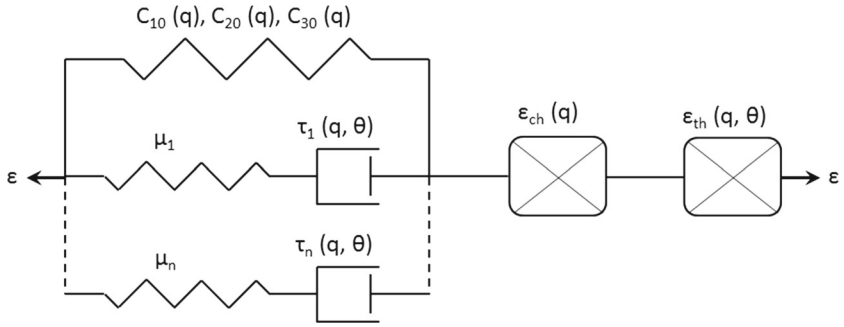

Fig. 8 Simplified rheological material model

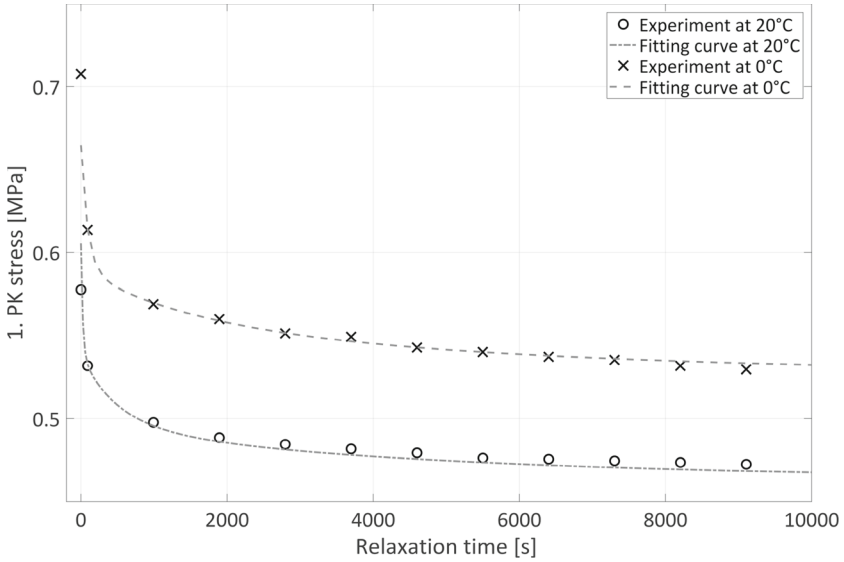

Fig. 9 Relaxation experiments at different temperatures used to fit the WLF parameters

The parameters fit to one relaxation experiment can be used to simulate the viscoelastic behavior at different temperatures as well, using the time–temperature shift according to Eq. 4a. The Maxwell elements' relaxation times τ_i are multiplied by the shift factor a_T as can be seen in Eq. 7. Figure 9 shows the curve fitting results using the parameters summarized in Table 2.

$$\tau_i(\theta) = \tau_i(\theta_\mathrm{ref}) \cdot a_\mathrm{T} \tag{7}$$

The specific enthalpy rate shown in the DSC curves (Fig. 2) does not show one distinctive reaction peak, but rather a blunt peak with a plateau that may be interpreted as a second peak. A curve shaped like this can be better described using a two-stage evolution equation. As a modeling approach, we assume there are two reactions which happen one after the other, with the material passing through an intermediate state when transitioning from fluid to solid. The evolution of the specific enthalpy rate $\dot{h}$ is modeled using two coupled evolution equations as proposed in [20]. The equations for the two partial degrees of curing q_p1 and q_p2 are modified differential equations of the Kamal–Sourour type (Eqs. 8a and 8b) containing Arrhenius terms k_i (Eq. 8c). In the standard Kamal–Sourour model, the sum of the exponents m and n determines the reaction order. The Arrhenius terms include the pre-exponential factors A_i, the universal gas constant R and the activation energies E_{ai} of the physically motivated model. The parameters do not retain their physical meaning as part of the two-stage evolution equation. The results are subsequently used to compute the specific enthalpy rate $\dot{h}$ by multiplying each partial degree of curing with an enthalpy ratio following Eq. 8d, where H_1 corresponds to the reaction enthalpy of the first partial reaction and H_{12} corresponds to the total reaction enthalpy.

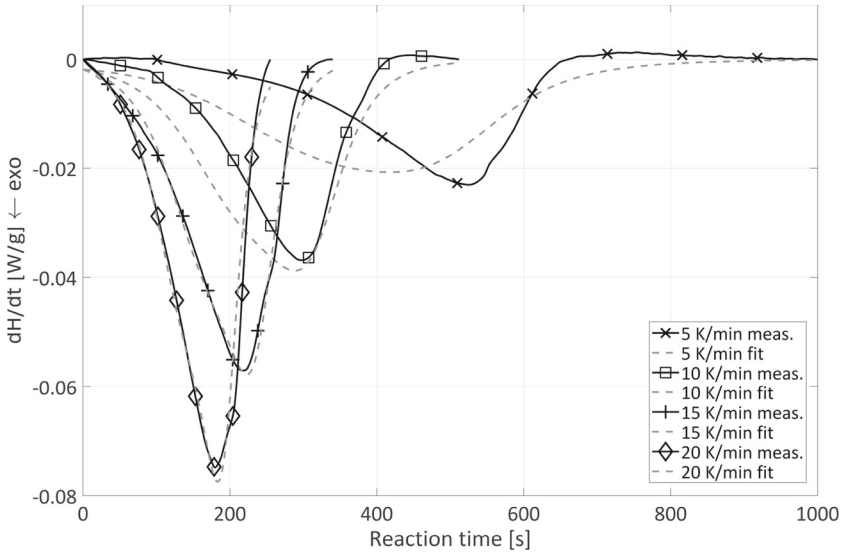

Fig. 10 Measurement curves and fitting curves of the specific enthalpy rate under different temperature rates over time

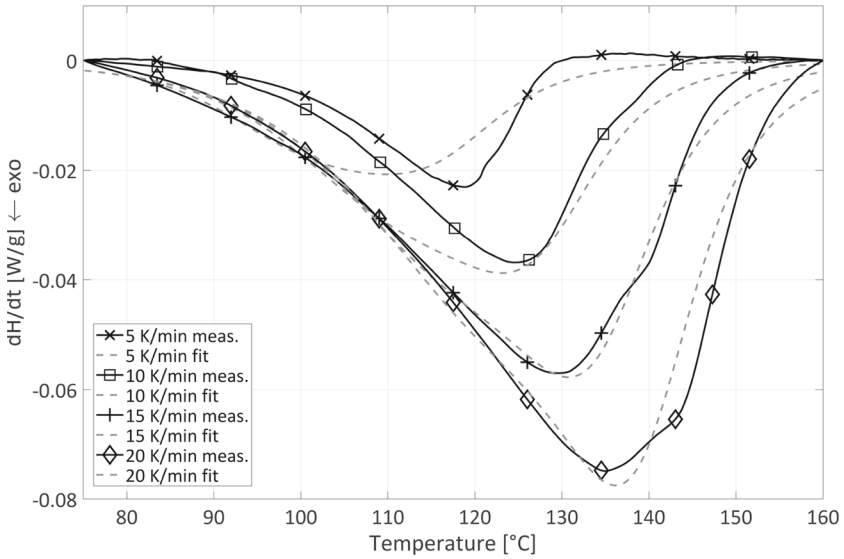

Fig. 11 Measurement curves and fitting curves of the specific enthalpy rate under different temperature rates over temperature

$$\dot{q}_{\mathrm{p1}} = [k_1 + k_2 \cdot (q_{\mathrm{p1}} - q_{\mathrm{p2}})^{m_1}] \cdot (1 - q_1)^{n_1} \tag{8a}$$

$$\dot{q}_{\mathrm{p2}} = [k_3 + k_4 \cdot {q_{\mathrm{p2}}}^{m_2}] \cdot (q_{\mathrm{p1}} - q_{\mathrm{p2}})^{n_2} \tag{8b}$$

$$k_i = A_i \cdot \mathrm{e}^{-\frac{E_{ai}}{R} \cdot \left(\frac{1}{\vartheta} - \frac{1}{\vartheta_{\mathrm{r}}}\right)} \tag{8c}$$

$$\dot{h} = H_{12} \cdot \left(\frac{H_1}{H_{12}} \cdot \dot{q}_{\mathrm{p1}} + \left(1 - \frac{H_1}{H_{12}}\right) \cdot \dot{q}_{\mathrm{p2}} \right) \tag{8d}$$

Figures 10 and 11 show the results of the parameter fitting. Both the self-acceleration effect and the deceleration effect when the reaction nears its end are well described. The parameters describing the curing reaction are listed in Table 3.

It is clear that the curing of the material and the subsequent transition from fluid to solid must also have an influence on its stiffness and viscosity. In a first approach, we assume the dependence to be linear as can be seen in Eqs. 9a and 9b. $c_{i0}^{q=1}$ are the Yeoh parameters of the fully cured material. Since it is a viscous fluid in

Table 3 Material parameters for modeling the curing reaction

Parameter	Value
A_1	$3.3 \times 10^{-6}\,\mathrm{s}^{-1}$
A_2	$7.6 \times 10^{-5}\,\mathrm{s}^{-1}$
A_3	$2.1 \times 10^{-7}\,\mathrm{s}^{-1}$
A_4	$1.5 \times 10^{-6}\,\mathrm{s}^{-1}$
E_{a1}	$9.4 \times 10^{4}\,\mathrm{J\,mol}^{-1}$
E_{a2}	$4.9 \times 10^{4}\,\mathrm{J\,mol}^{-1}$
E_{a3}	$3.1 \times 10^{4}\,\mathrm{J\,mol}^{-1}$
E_{a4}	$9.7 \times 10^{4}\,\mathrm{J\,mol}^{-1}$
m_1	0.6
m_2	2.6
n_1	1.3
n_2	1.7
H_1	$-1.2\,\mathrm{J\,g}^{-1}$
H_{12}	$-8.2\,\mathrm{J\,g}^{-1}$

its uncured state, the material is assumed to have no equilibrium stiffness. The relaxation times of the Maxwell elements need to be identified for the uncured ($\tau_i^{q=0}$) and the fully cured material ($\tau_i^{q=1}$).

$$c_{i0} = q \cdot c_{i0}^{q=1} \tag{9a}$$

$$\tau_i = \tau_i^{q=0} \cdot (1 - q) + \tau_i^{q=1} \cdot q \tag{9b}$$

4 Summary and outlook

The investigated polyurethane adhesive's special characteristic is its curing mechanism. It can cure either through temperature or through humidity, and one can affect the other as well. In Sect. 2.1, we introduced an approach to investigate the temperature curing through DSC experiments. While this approach is sufficient for a material that cures solely through temperature and we may describe the material behavior under conditions that exclude humidity curing quite well, additional experiments are necessary to analyze the humidity curing mechanism and the interactions between the two mechanisms. The mechanical properties of the fully temperature-cured material have been investigated extensively, the elastic, viscoelastic and temperature-dependent properties have been identified. The influences of the different curing mechanisms on the fully cured material need to be examined more closely once the full curing spectrum has been analyzed. Moreover, the dependence of the viscoelastic material properties on the degree of curing and the assumption made in Sect. 3 needs to be examined and validated by rheological experiments.

In conclusion, the approach outlined here already gives some insight into the experimental characterization of an adhesive with a complicated curing mechanism, but it is only the first step on the way to a material model that will be able to reproduce the material behavior in all stages of curing including the dependence on temperature, humidity and time. In the future, the uniaxial rheological model developed in this paper will be generalized to finite deformations and three-dimensional loadings.

Acknowledgements We would like to thank the Deutsche Forschungsgemeinschaft (DFG) (Grant No. LI696/17-1) for funding the research project from which this paper resulted.

References

1. Adolf, D.B., Chambers, R.S.: A thermodynamically consistent, nonlinear viscoelastic approach for modeling thermosets during cure. J. Rheol. **51**(1), 23–50 (2007)
2. Deutsches Institut für Normung e.V.: DIN 51007 Thermische Analyse (TA), Differenzthermoanalyse (DTA) (1994)
3. Enns, J.B., Gillham, J.K.: Time-temperature-transformation (TTT) cure diagram: modeling the cure behavior of thermosets. J. Appl. Polym. Sci. **28**(8), 2567–2591 (1983)
4. Fournier, J., Williams, G., Duch, C., Aldridge, G.A.: Changes in molecular dynamics during bulk polymerization of an epoxide-amine system as studied by dielectric relaxation spectroscopy. Macromolecules **29**(22), 7097–7107 (1996)

5. Grambow, A.: Bestimmung der Materialparameter gefüllter Elastomere in Abhängigkeit von Zeit, Temperatur und Beanspruchungszustand. Ph.D. thesis. RWTH Aachen (2002)
6. Hossain, M., Possart, G., Steinmann, P.: A finite strain framework for the simulation of polymer curing. Part I: elasticity. Comput. Mech. **44**(5), 621–630 (2009a)
7. Hossain, M., Possart, G., Steinmann, P.: A small-strain model to simulate the curing of thermosets. Comput. Mech. **43**(6), 769–779 (2009b)
8. Leistner, C., Hartmann, S., Abliz, D., Ziegmann, G.: Modeling and simulation of the curing process of epoxy resins using finite elements. Continuum Mech. Thermodyn. 1–24 (2018). https://doi.org/10.1007/s00161-018-0708-9
9. Leistner, C., Hartmann, S., Wittrock, J., Bode, K.: Shrinkage behavior of araldite epoxy resin using archimedes' principle. Polym. Test. **67**, 409–416 (2018b)
10. Liebl, C.: Viskoelastisch-viskoplastische Modellierung von Strukturklebstoffen während der Aushärtung. Ph.D. thesis. Bundeswehr University Munich (2014)
11. Lion, A.: Einführung in die lineare viskoelastizität. In: Beiträge zur Materialtheorie. A. Lion (2007)
12. Lion, A., Höfer, P.: On the phenomenological representation of curing phenomena in continuum mechanics. Arch. Mech. **59**(1), 59–89 (2006)
13. Mahnken, R.: Thermodynamic consistent modeling of polymer curing coupled to visco-elasticity at large strains. Int. J. Solids Struct. **50**(13), 2003–2021 (2013)
14. Pahl, M., Gleißle, W., Laun, H.M.: Praktische Rheologie der Kunststoffe und Elastomere. VDI-Gesellschaft Kunststofftechnik (1991)
15. Rabearison, N., Jochum, C., Grandidier, J.C.: A cure kinetics, diffusion controlled and temperature dependent, identification of the araldite ly556 epoxy. J. Mater. Sci. **46**(3), 787–796 (2011)
16. Shutov, A.V., Landgraf, R., Ihlemann, J.: An explicit solution for implicit time stepping in finite strain viscoelasticity. Comput. Methods Appl. Mech. Eng. **265**, 213–225 (2013)
17. Sourour, S., Kamal, M.R.: Differential scanning calorimetry of epoxy cure: isothermal cure kinetics. Thermochimica Acta **14**, 41–59 (1976)
18. Williams, M.L., Landel, R.F., Ferry, J.D.: The temperature dependence of relaxation mechanisms in amorphous polymers and other glass-forming liquids. J. Am. Chem. Soc. **77**, 3701–3707 (1955)
19. Yagimli, B.: Kontinuumsmechanische Betrachtung von Aushärtevorgängen. Ph.D. thesis. Bundeswehr University Munich (2013)
20. Yagimli, B., Lion, A.: Experimental investigations and material modelling of curing processes under small deformations. J. Appl. Math. Mech. **91**(5), 342–359 (2011)
21. Yeoh, O.H., Fleming, P.D.: A new attempt to reconcile the statistical and phenomenological theories of rubber elasticity. J. Polym. Sci. **35**(12), 1919–1931 (1997)